NASA Technical Memorandum 102291

Friction and Wear of Oxide-Ceramic Sliding Against IN-718 Nickel Base Alloy at 25 to 800 °C in Atmospheric Air

Harold E. Sliney and Daniel L. Deadmore
Lewis Research Center
Cleveland, Ohio

August 1989

NASA

FRICTION AND WEAR OF OXIDE-CERAMICS SLIDING AGAINST IN-718 NICKEL BASE ALLOY AT 25 TO 800 °C IN ATMOSPHERIC AIR

Harold E. Sliney and Daniel L. Deadmore
National Aeronautics and Space Administration
Lewis Research Center
Cleveland, Ohio 44135

SUMMARY

The friction and wear of oxide-ceramics sliding against the nickel base alloy IN-718 at 25 to 800 °C were measured. The oxide materials tested were mullite ($3Al_2O_3 \cdot 2SiO_2$); lithium aluminum silicate ($LiAlSi_xO_y$); polycrystalline monolithic alpha alumina (α-Al_2O_3); single crystal α-Al_2O_3 (sapphire); zirconia (ZrO_2); and silicon carbide (SiC) whisker-reinforced Al_2O_3 composites. At 25 °C the mullite and zirconia had the lowest friction and the polycrystalline monolithic alumina the lowest wear. At 800 °C the Al_2O_3-8 vol % SiC whisker composite had the lowest friction and the Al_2O_3-25 vol % SiC composite the lowest wear.

The friction of the Al_2O_3-SiC whisker composites increased with increased whisker content while the wear decreased.

In general, the wear-resistance of the ceramics improve with their hardness.

INTRODUCTION

Oxide-ceramic materials are currently receiving attention for use in high temperature areas of heat engines and other energy conversion systems (ref. 1). These materials are candidates for cylinder liners, piston caps and other uses. In some applications, sliding or rubbing contact with themselves or other materials, such as metal alloys, can be expected.

Oxide-ceramics studied in this program are mullite ($3Al_2O_3 \cdot 2SiO_2$); lithium aluminum silicate ($LiAlSi_xO_y$); polycrystalline monolithic alpha alumina (α-Al_2O_3); single crystal Al_2O_3 (sapphire); Al_2O_3 matrix composite containing SiC whiskers; and ZrO_2.

The purpose of this investigation was to measure the friction and wear of the oxide-ceramics in unlubricated sliding contact with the nickel base alloy IN-718 at 25 to 800 °C in atmospheric air. A load of 6.8 kg (67N) and a linear sliding velocity of 0.5 m/sec for 60 min was used. Testing was done on a double rub block test machine with line contact of the static oxide-ceramic rub blocks against the circumferential surface of a rotating IN-718 disk. Friction and wear were determined, and the sliding surfaces were examined by SEM (Scanning Electron Microscopy), EDS (Energy Dispersive X-Ray Spectroscopy) and WDS (Wavelength Dispersive X-Ray Spectroscopy).

EXPERIMENTAL

Test Apparatus

A double rub block-line contact wear and friction apparatus was used for all tests. Figure 1(a) is a photograph of the loading and rub block support fixture. Two rub blocks are pressed against the rotating disk by pressurizing the bellows, and the frictional torque is transmitted via the torque arm to a measuring and support system. The blocks are initially in nominal line contact with the disk. Uniform loading along this line is maintained by the pivoted, self-aligning block holders. The disk is 3.492 cm diameter and 1.28 cm thick, and the rub blocks are 2.22 cm long by 0.63 cm wide and 1.11 cm deep. The torque system is calibrated with dead weights. A schematic diagram of the induction heating coil and sleeves used to bring the disk to the test temperature is presented in figure 1(b). The temperature of the disk surface is measured by an optical pyrometer.

All determinations are made in atmospheric air at ambient pressure with a relative humidity of 45 to 60 percent. Each rub block is loaded to 6.8 kg (67N). The sliding velocity is 0.5 m/sec. All tests were run for 60 min unless otherwise indicated.

Cleaning Procedure

The test specimens are thoroughly cleaned before each experiment. The IN-718 disks are first polished with a dry felt cloth and levigated alumina then rinsed with distilled water. They are then scrubbed with a paste of levigated alumina and water, rinsed with distilled water and finally cleaned by scrubbing with ethanol. The ceramic rub blocks are cleaned with only an ethanol rinse to remove surface films. Polishing with alumina is omitted to avoid possible imbedding of polishing compound particles in the surface of some ceramics, such as mullite, that exhibited surface porosity.

Friction and Wear Experiments

The disk and rub block specimens are assembled into the test apparatus and induction heated to the planned test temperature. The disk is rotated during heating to insure a uniform temperature distribution over its outer rim (wear surface). After the specimen temperature has stabilized at the test temperature, the rub blocks are pressed against the disk under a known load by pressurizing the calibrated load bellows. Friction force is measured and recorded continuously.

After each test, the specimens are allowed to cool; they are then removed from the test apparatus, and their volumetric wear is measured. Wear areas are determined by obtaining stylus profilometer traces transverse to the disk wear track and to the rub shoe wear scars. Disk wear volume is computed by multiplying the wear areas across the track by the disk circumference. Rub block wear is obtained by multiplying the wear scar cross sectional area by the block width. Wear areas for each specimen are taken as the average from profilometer traces taken at four locations on the disk and three locations (one at each end and one at the center) of each rub block.

A wear factor, K, is calculated from each wear volume. It is a measure of the average wear volume per unit load, per unit distance of sliding and is expressed in units of:

$$K = \frac{mm^3 \text{ (wear volume)}}{\text{Newton(load) x meter (sliding distance)}} \text{ or } \frac{mm^3}{Nm}$$

Material Characterization

The analytical techniques used to characterize the materials are described in detail in references. 2 to 4). In brief, they consist of:

1. Scanning Electron Microscopy (SEM) along with:
   a. Energy dispersive x-ray spectroscopy (EDS) for analysis of elements of atomic number greater than 12 (Mg)
   b. Wavelength dispersive x-ray spectroscopy (WDS) for the lighter elements
   c. A quantitative analyses program (NOSTD) which does not employ standards, but does make corrections for atomic number (Z), x-ray absorption (A), and fluorescence (F)
2. X-Ray Diffraction (XRD)
3. Vickers hot hardness measurements

These techniques are used to characterize the materials before the tribotests and to study wear surfaces after the tests. Figure 2 illustrates the areas chosen for analyses on worn rub blocks and disks.

Starting Materials

A listing of typical composition and physical properties of the starting materials are presented in table I. Most of the ceramics are not pure or fully dense but contain other constituents or phases and have some degree of porosity.

Mullite

Mullite is a mineralogical name for the stoichiometric composition $3Al_2O_3$-$2SiO_2$. The material tested here is called mullite but is a commercial material composed of a mixture of mullite and other phases. A photomicrograph of the polished and unetched material is presented in figure 3. The structure is that of a light gray elongated crystalline appearing material dispersed in a darker gray matrix. The EDS spot analysis of the crystalline appearing phase reveal a high Al and Si content which is comparable to the spectrographic bulk analysis given in table I. However, Al is lower than that calculated for pure, stoichiometric $3Al_2O_3$-$2SiO_2$ and Si is higher. This indicates that the crystalline phase is a mixture of mullite and SiO_2. XRD gives a pattern for mullite only, which suggests the SiO_2 is noncrystalline. The matrix is a high silica phase containing K, Ti and Fe in relatively large amounts suggesting it is a silica rich glassy phase. In brief, the structure of this material is that of crystalline matter cemented together by a silica glass. This is typical of many ceramic materials.

This material has a high porosity with a density that is only 84 percent of the true density given in table I. Numerous pores are clearly present in the low magnification photomicrographs presented in figures 3 and 4(a). This high porosity contributes to a high average surface roughness of 1 to 1.25 μm. This is the roughest surface of all of the materials tested.

Lithium-Aluminum-Silicate

This is a commercial, polycrystalline material composed of Li, Al, Si and oxygen. The spectrographic bulk analysis reveals that Li, Al, and Si and small amounts of Ti and Fe are present. The chemical analysis and XRD pattern both suggest a formula of $LiAlSi_xO_y$ where X=2 to 3 and Y=6 to 8. This is in the region of the Li_2O, Al_2O_3, SiO_2 phase diagram for beta-spodumene. This material and other compositions in this phase diagram possess very low thermal expansion, in fact, some compositions exhibit negative values. Low expansion coefficients give these materials a high degree of resistance to physical degradation by thermal shock.

The photomicrograph in figure 4(b) reveals a high degree of porosity with many large pores. The high porosity produces a large average surface roughness of 0.62 to 0.75 μm which is only somewhat less than that of the mullite. This material has the lowest hardness of all the materials tested.

Aluminum Oxide

This material is a sintered, polycrystalline, high purity, low porosity material procured from a commercial producer. Spectrographic analysis of this material indicates that it is about 99 percent Al_2O_3 with trace amounts of Fe_2O_3 and TiO_2. The XRD pattern revealed an alpha-alumina crystal structure. A photomicrograph at high magnification is presented in figure 5(a). It is evident that some porosity is present at the grain boundaries. The ratio of the bulk to true density is about 95 percent. The surface finish is 0.25 to 0.38 μm.

Aluminum Oxide-Silicon Carbide Composite

These materials are commercially available polycrystalline Al_2O_3 containing 8, 15, and 25 vol % SiC whiskers. Photomicrographs of these composites are presented in figures 5(b) to (d). The SiC whiskers are easily detected and are 0.25 to 1.25 μm diameter and 5 to 12 μm long.

XRD patterns reveal alpha-alumina and alpha-SiC. These composites have low porosity and thereby have some of the best surface finishes (0.1 to 0.2 μm) of all the materials tested.

Sapphire

This is a very high purity, low porosity, transparent, single crystal Al_2O_3. The sliding test surface is the (1, 0, 10) orientation. The XRD pattern reveals only alph-alumina. The polished surface roughness is 0.3 to 0.4 μm.

Zirconia

The ZrO_2 studied is a partially stabilized, transformation toughened material. It is commercially produced and is designated by the manufacturer as the MS (maximum strength) grade. The stabilizers are MgO and HfO_2. The XRD pattern reveals it to be a mixture of monoclinic and cubic ZrO_2. The vendor literature describes the microstructure as consisting of monoclinic, tetragonal and cubic ZrO_2. The matrix is cubic with fine ellipsoidal shaped tetragonal precipitates uniformly distributed in the cubic grains. A monoclinic phase also exists within these grains and at the grain boundaries. This material has a porosity of 1 to 2 percent which can be seen as fine pores or voids in figure 4(c). Its fracture toughness and strength as reported by the vendor are even higher than those of the whisker reinforced Al_2O_3 composites.

IN-718 Alloy

Alloy IN-718 is a nickel based material with a nominal composition of Ni 53, Cr 18.5, Fe 18.5, Nb 5, Mo 3.1, Ti 0.9, Al 0.4, Si 0.3, Mn 0.2, and C 0.04 wt %. The Vickers hardness of this alloy at 25.C is 517± 4 kg/mm^2 at 100 g load. The surface finish (Ra) is 0.2 μm.

RESULTS AND DISCUSSION

Friction

Typical friction coefficients for the various ceramics sliding on Inconel 718 are presented in table II and plotted against temperature in figures 6 and 7. The deviation is ±0.04. In general the friction coefficients of unlubricated monolithic oxides sliding against IN-718 decrease with increase in temperature down to about 0.3 at 800 °C.

Figure 7 reveals that, as in the case of the monolithic ceramics, the sliding friction of the alumina-SiC composites are high, 0.4 to 0.5, at 25 °C and decreases to 0.25 to 0.3 at 800 °C. The sapphire, polycrystalline alumina and the 8 vol % SiC composite all follow nearly the same response to temperature while the 15 and 25 vol % composites show higher friction especially at lower temperatures. It was reported in reference 3 that the friction of monolithic SiC sliding on IN-718 is very high (0.62) at 25 °C and 0.56 at 350 °C. This high friction for SiC may be the reason for the higher friction of the 15 and 25 vol % SiC composites.

It has been reported that the friction of metals sliding against each other in an atmosphere containing oxygen is less than in an oxygen free atmosphere (ref. 5). It was found in the former case that a thin, lubricious oxide layer formed that was responsible for the lower friction in an oxidizing atmosphere. In the present work, the decrease in friction for ceramics sliding against IN-718 at elevated temperatures is also due to the formation of a lubricious oxide layer. The oxide is formed on the metal and subsequently transferred to the ceramic during sliding.

The oxide transfer film is readily observed visually, and was also quantitatively analyzed by EDS. The concentration of transferred nickel divided

by the concentration of an element of the ceramic rub block material gives an indication of the degree of material transfer to the ceramic surface. Ceramic transfer from the rub blocks to the metal disk is determined in an analagous fashion. These concentration ratios are given in table II. In the case of metal transfer, only nickel transfer is reported, but all of the other alloy elements were found to be present in the transferred film in the same proportion as in the alloy, thus indicating no preferential element transfer. The nickel/ceramic element ratio is higher on the ceramic rub blocks tested at elevated temperatures where the transferred metal is oxidized. This is consistent with the mechanism that attributes the reduction in friction coefficient at elevated temperatures to the presence of a lubricative film of alloy oxide on the ceramic surface.

Similar data for transfer of ceramic from the rub blocks to the disk show that little or no transfer occurs in that direction. In table II, the oxygen content inside and outside of the wear track on the disk is given as a ratio, R. When this ratio is greater than one it indicates that the oxygen content of the surface in the wear track is higher than outside. At the lower test temperatures, this ratio is much greater than one in spite of the fact that the oxide is wearing away and transferring to the ceramic during sliding. By 800 °C the ratio is essentially one and the oxygen inside and outside the wear track is the same. This trend indicates that the oxidation rate of the metal in the wear track is much higher than it is in the static, isothermal areas outside of the wear track. This is almost certainly due to the higher temperatures induced in the wear track by frictional heating. The influence of frictional heating on the oxidation rate becomes less pronounced at 800 °C. This is possibly because frictional heating is a small percentage of the total heat input at that temperature and the friction coefficient itself (and therefore frictional heating) tends to decrease with temperature.

WEAR

Monolithic Ceramics Sliding on IN-718 Alloy

Wear data are tabulated in table II and presented graphically in figures 8 to 12.

Figure 8 gives wear data for the monolithic ceramic/IN-708 sliding combinations. The most apparent trend in figure 8(a), which presents the wear factors for the ceramic rub blocks, is that wear decreases markedly with increasing temperature. The wear factor for lithium aluminum silicate is in the high wear regime at room temperature but decreases to the low wear regime at 800 °C. The other ceramics are in the moderate wear regime at room temperature and this decreases to low wear at 800 °C.

The corresponding wear of the metal disks as a function of temperature is given in figure 8(b). The trends in metallic wear are not as orderly as they are for ceramic wear. For most of the sliding combinations, the wear factors are at a minimum between 500 and 600 °C. Metallic wear is typically in the moderate to low regime. The potential usefulness of a slider material combination depends on the total wear of the materials. If we add the ceramic and metallic wear factors to obtain the total wear factors for each combination of slider materials, we find some combinations, such as alumina and IN-718, for

which ceramic wear is low, but total wear may be unacceptably high (see fig. 12). Monolithic ceramics that give reasonably low total wear at both room temperature and at 800 °C when sliding against IN-718 are mullite and zirconia.

Silicon Carbide-Alumina Composites Sliding on IN-718

Silicon carbide whisker-reinforced alumina composites of various whisker contents were evaluated. Figure.9 presents wear factors for the ceramic composite rub blocks and the IN-718 disks from 25 to 800 °C. Wear factors for all of the composite rub blocks decrease as the test temperatures are increased. At any given temperature the wear factors decrease with increasing whisker content. However, no clear trend exists for wear of the metal disks. The wear data cluster at 25 and 800 °C in an apparently random manner. At 350 and 550 °C, metallic wear is higher for sliding on the alumina composites then it is on monolithic alumina.

Mechanical properties supplied by the vendor are presented in figure 10(a). Four point bend strength and fracture toughness are given as a function of whisker content. Wear data for these composites are presented in figure 10(b). A comparison of the wear data with the mechanical properties data strongly suggests that the decrease in wear is due to the increase in strength and fracture toughness provided by the silicon carbide whiskers. This is in agreement with the data in figure 11 (refs. 6 and 7) that show the effect of fracture toughness on the wear resistance of ceramics and metals. The wear of ceramics is generally controlled by a fracture mechanism; therefore wear resistance is seen to increase with increased fracture toughness. Unfortunately as previously stated, the friction coefficients also increase with increased silicon carbide whisker content above 8 vol %.

Figure 12 compares the total ceramic plus metallic wear for the monolithic ceramics and the silicon carbide-alumina composites. It can be seen that although the wear of the composites is very low, these materials are more abrasive to the metal counterfaces than the monolithic ceramics and the total wear is the same order of magnitude as it is for some of the monolithic ceramic/IN-718 combinations. The lowest total wear at room temperature was obtained with mullite, alumina with 15 vol % SiC, alumina with 8 vol % SiC, and zirconia. The lowest total wear at 800 °C was obtained with mullite, lithium aluminum silicate, alumina with 8 vol % SiC, and zirconia.

The Effect of Microhardness on Wear

Microhardness measurements of the ceramics studied in this investigation were made at 25 to 800 °C. The wear factors as a function of hardness are plotted in figure 13; the solid lines are least squares fits to the data. Some of the wear and hardness data are from our previous work reported in references 3 and 4. The wear factors decrease at both temperatures as the hardness increases. Therefore, the wear resistance of these materials correlates with their hardness as well as with their previously-discussed fracture toughness.

Macro-Appearance of Ceramic Rub Surfaces

Photographs of the wear scars on the ceramic rub blocks are presented in figures 14 to 21. The relative extent of wear is clearly evident. In cases of severe wear, the scars tended to be unsymmetrical with more wear occurring on one side than the other. In those cases, the average wear was used to calculate the wear factors.

CONCLUSIONS

An investigation of the unlubricated friction and wear of oxide ceramics sliding against IN-718 nickel base alloy in air at temperatures from 25 to 800 °C and a sliding velocity of 0.5 m/sec led to the following conclusions.

1. The friction coefficients of all ceramics studied in sliding contact with IN-718 are in the range of 0.4 to 0.5 at room temperature. Friction coefficients decrease steadily with temperature to 0.24 to 0.30 at 800 °C. Visual and quantitative surface analyses show that during sliding at elevated temperatures, the metal specimen oxidizes and transfers some of the oxide to the ceramic surface where it forms a tenacious film which has a lubricating effect that is responsible for the reduction in friction.

2. In general, the wear-resistance of the ceramics improve with their fracture toughness and their hot hardness. However, some of the most wear-resistant ceramics cause higher wear of the counterface metal than the softer ceramics. This results in total wear of the sliding system that in some cases is higher than that seen with a softer ceramic.

3. The mullite form of aluminum silicate is relatively soft with a Vickers hardness of 900 at room temperature and 450 at 800 °C, but because it is less abrasive than some of the harder ceramics to the metal counterface, the lowest total system wear is obtained with the mullite/IN-718 pair from 25 to 800 °C. A disadvantage of mullite is the difficulty in obtaining high density material. The porosity commonly present in mullite is the source of many failure initiation sites, that result in a low strength material. The results of this study therefore suggest that a low porosity mullite is potentially an attractive high temperature sliding contact bearing material.

4. Silicon carbide whisker-reinforced aluminum oxide is much stronger and has better wear resistance than the monolithic ceramics studied in this program. Both mechanical strength and wear-resistance improve with increasing whisker content. However, metal counterface wear can be higher than it is for some of the monolithic ceramics, and total system wear is not necessarily improved by using the strongest of these composite ceramics. Also, friction coefficients tend to increase with increasing whisker content.

5. A good compromise between high strength and low total system wear appears to be the use of an alumina composite with 8 vol % silicon carbide whisker content. This material has excellent wear-resistance, is only slightly more abrasive to IN-718 than mullite, and exhibits friction coefficients slightly lower than mullite above 500 °C, but higher than mullite at 25 and 350 °C.

6. From a consideration of tribological properties alone, the mullite/IN-718 combination is the best with the lowest wear from 25 to 800 °C and the most favorable overall friction coefficients.

REFERENCES

1. Kaminsky, M.; and Michaels, A.E., eds.: Tribology Project. Energy Conversion and Utilization Technologies Division, Quarterly Progress Report, Jan.-Mar. 1985, TRIB-ECUT-85-2, DOE, Apr. 1985.

2. Deadmore, D.L.; and Sliney, H.E.: Hardness of CaF_2 and BaF_2 Solid Lubricants at 25 to 670 °C. NASA TM-88979, 1987.

3. Deadmore, D.L.; and Sliney, H.E.: Friction and Wear of Sintered Alpha SiC Sliding Against IN-718 Alloy at 25 to 800 °C in Atmospheric Air at Ambient Pressure, NASA-TM-87353, 1986.

4. Deadmore, D.L.; and Sliney, H.E.: Friction and Wear of Monolithic and Fiber Reinforced Silicon-Ceramics Sliding Against IN-718 Alloy at 25 to 800 °C in Atmospheric Air at Ambient Pressure. NASA TM-100294, 1988.

5. Stott, F.H.; and Wood, G.C.: The Influence of Oxides on the Friction and Wear of Alloys. Tribology Int., vol. 11, no. 4, Aug. 1978, pp. 211-218.

6. Hornbogen, E.: Description of Wear of Materials With Isotropic and Anisotropic Microstructures. Wear of Materials, K.C. Ludema, ed., ASME, 1985, pp. 477-484.

7. Hornbogen, E.: The Role of Fracture Toughness in the Wear of Metals. Wear, vol. 33, no. 2, July 1975, pp. 251-259.

TABLE I. - COMPOSITION AND PROPERTIES OF OXIDE CERAMIC RUB BLOCKS BEFORE TEST

Material	Composition	Phases detected by XRD	Tested surface roughness	Bulk den·g/cm^3	Vickers hardness at 25 °C (kg/mm^2)[d]	Other Properties[b]			
						Bend strength		Fracture toughness	
						MPa	psi	MPa-m$^{1/2}$	kpsi-in$^{1/2}$
Mullite (Sintered)	27.5Al, 0.3Fe[a] 19.1Si, 0.5Ti	Mullite ($3Al_2O_3 \cdot 2SiO_2$)	40–50 μin (1–1.25 μm)	2.70[c] ≈84 percent TD[e]	926±56[c] (100 g load)	(-)	(-)	(-)	(-)
LiAl Silicate (Sintered)	10Al, <0.05 ppm Fe[a] 38.5Si, <0.03 ppm Ti 1.5Li	$LiAlSi_xO_y$ (x=2–3) (y=6–8) (β-spodumene)	25–30 μin (0.62–0.75 μm)	2.28c	489±58[c] (100 g load)	(-)	(-)	(-)	(-)
Al_2O_3 (Polycrystalline sintered)	52.6Al, <0.05 ppm Fe[a] <0.03 ppm Ti	α-Al_2O_3	10–15 μin (0.25–0.38 μm)	3.78[c] ≈95 percent TD[e]	1607±8[c] (100 g load)	(-)	(-)	(-)	(-)
Al_2O_3–8 vol % SiC whiskers (sintered)	8 vol % SiC 92 vol % Al_2O_3	αAl_2O_3 α-SiC	6–8 μin (0.15–0.2 μm)	3.84[c] 3.80[b]	1747±63[c] (100 g load) 2050[b]	414	60 000	5.5	5
Al_2O_3–15 vol % SiC whiskers (hot pressed)	15 vol % SiCb 85 vol % Al_2O_3	α-Al_2O_3 α-SiC	5–6 μin (0.12–0.15 μm)	3.83[c] 3.80[b]	2024±132[c] (100 g load) 2075[b]	586	85 000	7.7	7
Al_2O_3–25 vol % SiC whiskers (hot pressed)	25 vol % SiC[b] 75 vol % Al_2O_3	α-Al_2O_3 α-SiC	4–5 μin (0.1–0.12 μm)	3.73[c] 3.74[b]	2193±30[c] (100 g load) 2125[b]	641	93 000	8.8	8
Sapphire (single crystal)	99.8Al_2O_3[a]	α-Al_2O_3 (1,0,10) orientation)	12–16 μin (0.3–0.4 μm)	3.97[c] 3.99[b]	1955±149[c] (100 g load)	(-)	(-)	(-)	(-)
ZrO_2 PSZ (MS-grade) (sintered)	HFO_2 2–3 wt %[b] MgO 3.3–3.4 SrO 0.25 max TiO_2 0.15 Al_2O_3 0.03 Fe_2O_3 120 ppm	Cubic ZrO_2 Monoclinic ZrO_2	4–5 μin (0.1–0.12 μm)	5.64[c] 5.74[b] (1–2 percent porosity	1175±149[c] (100 g load) 1120[b]	725	104 000	8–12	(-)

[a]Spectrographic Analysis (weight percent unless noted otherwise).
[b]Vendor results.
[c]Present results.
[d]Hardness with standard deviation.
[e]Percent of theoretical density.

TABLE II. - FRICTION, WEAR AND MATERIAL TRANSFER DURING SLIDING OF OXIDE CERAMICS ON IN-718 NICKEL BASE ALLOY

[Air atmosphere (40 to 60 percent R.H.), 67N load power rub block, 0.5 m/s sliding velocity, 60 min. duration.]

Sliding couple		Test temperature, °C	Wear factor(mm^3/N-M)		Alloy element trans. to rub block			Ceramic element trans. to disk			Oxygen ratio on disk R(a)	Avg. coeff. of friction at 1800 m of sliding
Disk material	Rub block material		Disk	Rub block	Ni/Al	Ni/Si	Ni/Zr	Al/Ni	Si/Ni	Zr/Ni		
IN-718	Al_2O_3 (polycryst.)	25	6.5×10^{-5}	2.5×10^{-5}	51	———	———	0	———	———	3.8	0.44
		350	3.3×10^{-6}	4×10^{-6}	>100	———	———	0	———	———	2.2	.35
		550	7.2×10^{-6}	1×10^{-6}	>100	———	———	0	———	———	2.7	.28
		800	1.8×10^{-5}	2×10^{-7}	>100	———	———	0	———	———	1.3	.27
IN-718	Al_2O_3 (sapphire)	25	(b)	(b)	2.4	———	———	———	———	———	—	0.43
		350	3.7×10^{-5}	5.5×10^{-6}	41	———	———	———	———	———	—	.35
		550	1.9×10^{-6}	1.7×10^{-6}	89	———	———	———	———	———	—	.30
		800	6.8×10^{-6}	6×10^{-7}	>100	———	———	———	———	———	—	.25
IN-718	Al_2O_3 8 vol % SiC whiskers	25	4.1×10^{-5}	6×10^{-6}	138	———	———	0	———	———	2.2	0.46
		350	4.2×10^{-5}	2.5×10^{-6}	>100	———	———	0	———	———	4.7	.33
		550	1.4×10^{-5}	9.8×10^{-7}	>100	———	———	0	———	———	2.8	.28
		800	7.1×10^{-6}	4.6×10^{-8}	>100	———	———	0	———	———	0.9	.24
IN-718	Al_2O_3 15 vol % SiC whiskers	25	4.2×10^{-5}	2.6×10^{-6}	>100	———	———	———	———	———	—	0.48
		350	3.3×10^{-5}	1.4×10^{-6}	>100	———	———	———	———	———	—	.40
		550	2.7×10^{-5}	6.9×10^{-7}	>100	———	———	———	———	———	—	.3
		800	1.3×10^{-5}	3.4×10^{-8}	>100	———	———	———	———	———	—	.25
IN-718	Al_2O_3 25 vol % SiC whiskers	25	5×10^{-5}	1.6×10^{-6}	>100	———	———	———	———	———	2.4	0.52
		350	3×10^{-5}	1.5×10^{-6}	>100	———	———	———	———	———	1.2	.45
		550	8.3×10^{-5}	1.8×10^{-7}	>100	———	———	———	———	———	2.0	.34
		800	1.7×10^{-5}	2.4×10^{-8}	>100	———	———	———	———	———	1.0	.28
IN-718	Mullite	25	3.7×10^{-6}	4.1×10^{-5}	8.3	5.2	———	0.003	0.006	———	3.1	0.38
		350	2.8×10^{-6}	4.9×10^{-6}	32	19	———	0	0	———	3.4	.3
		550	1.4×10^{-6}	9.7×10^{-7}	>100	>100	———	0	0	———	1.9	.3
		800	3.6×10^{-6}	2.1×10^{-7}	>100	>100	———	0	0	———	0.9	.3
IN-718	LiAlSil	25	1.9×10^{-5}	5×10^{-4}	>100	0.9	———	0	0.02	———	2.6	.55
		350	1.8×10^{-5}	2.1×10^{-4}	>100	2.9	———	0	.03	———	2.5	.30
		550	2.5×10^{-6}	1.5×10^{-5}	>100	20	———	0	.005	———	1.0	.50
		800	4.8×10^{-6}	1.1×10^{-6}	>100	>100	———	0	0	———	1.3	.26
IN-718	ZrO_2 PSZ	25	1.3×10^{-6}	4.5×10^{-5}	———	———	0.03	———	———	0.13	2.2	.38
		800	5.6×10^{-6}	4.6×10^{-7}	———	———	.4	———	———	.01	.74	.28

[a]Ratio of oxygen inside the wear track to that outside the wear track after test.
[b]Rub block fractured and terminated the test after 8 min.

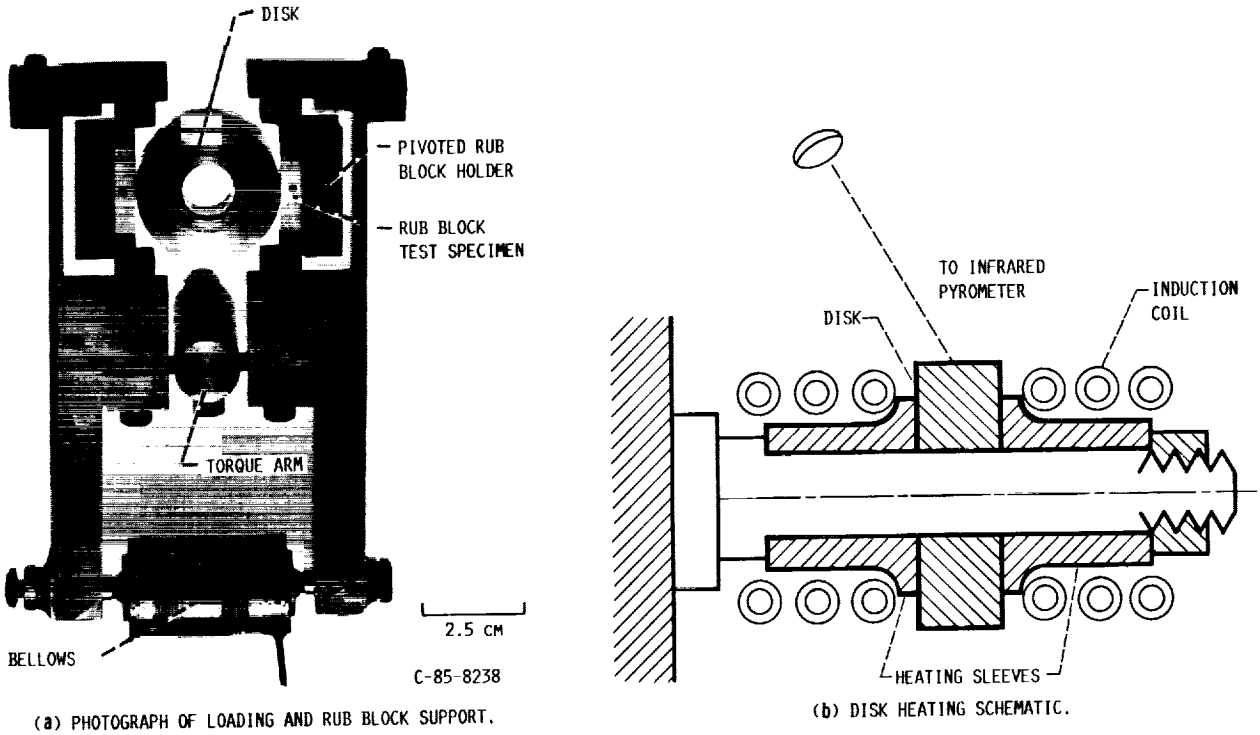

(a) PHOTOGRAPH OF LOADING AND RUB BLOCK SUPPORT.

(b) DISK HEATING SCHEMATIC.

FIGURE 1. - DOUBLE RUB BLOCK FRICTION AND WEAR TESTER.

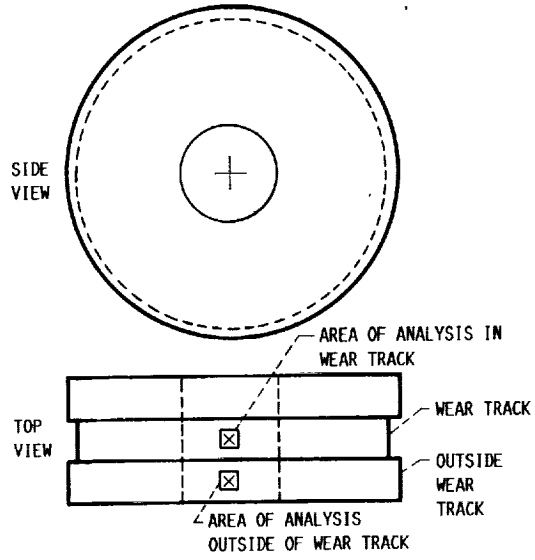

(a) DISK.

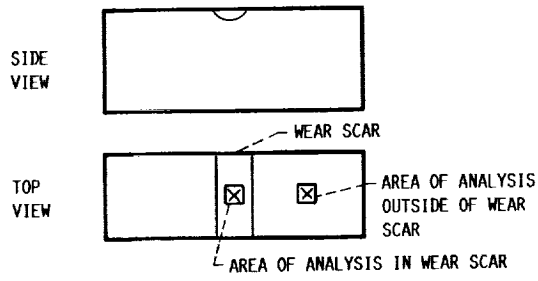

(b) RUB BLOCK.

FIGURE 2. - AREAS OF EDS AND WDS ANALYSIS ON DISKS AND RUB BLOCKS.

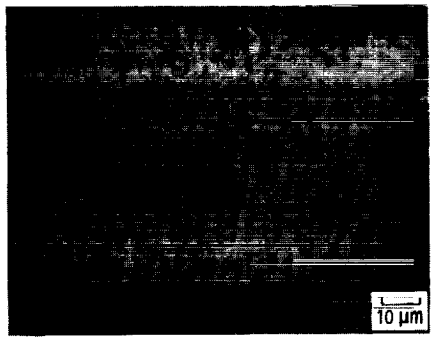

(a) EDX OF MATRIX AND GRAY CRYSTALS.

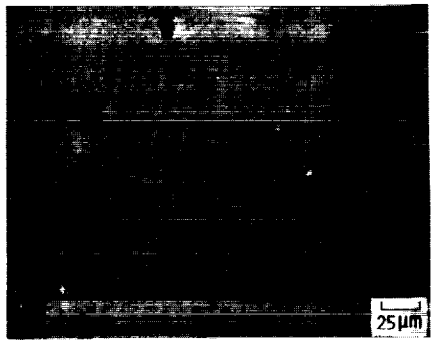

(b) PHOTOMICROGRAPH OF MULLITE.

SPOT	Al	Si	K	Ti	Fe
A DARK GRAY MATRIX	26	58	8	4	4
B LITE GRAY CRYSTALS	62	36	0.2	1.1	0.7
MULLITE*	74	26	0	0	0
BULK ANALYSIS (TABLE 1)	58	40.3	-	1.1	0.6

FIGURE 3. - PHOTOMICROGRAPHS OF MULLITE POLISHED AND UNETCHED. *CALCULATED FOR THE 3 Al_2O_3-2SiO_2 MULLITE COMPOSITION.

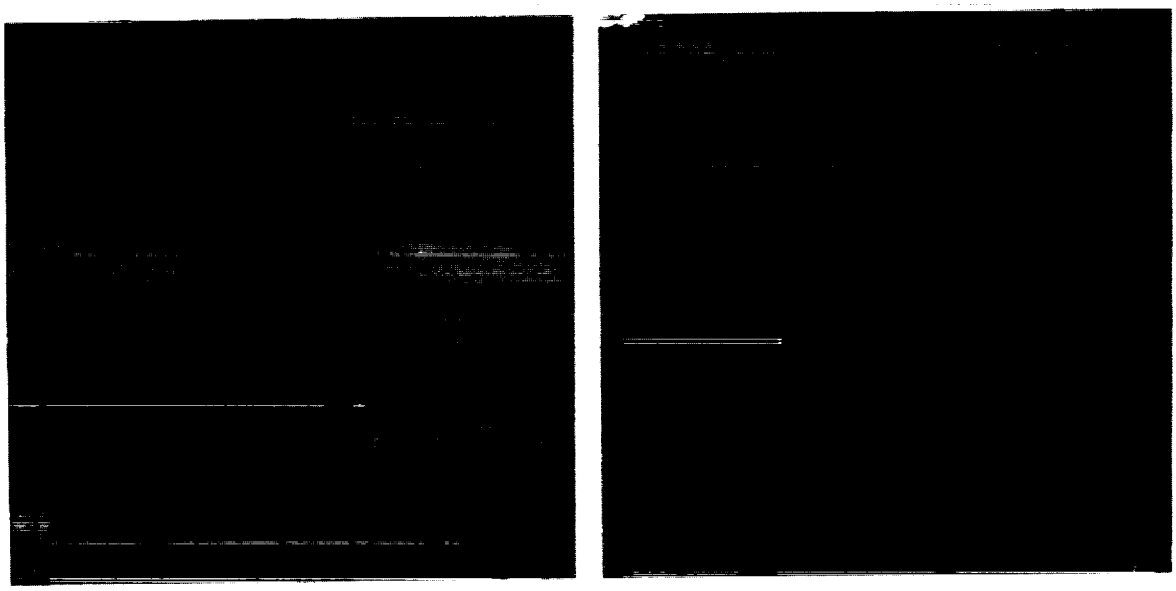

(a) MULLITE. (b) LiAlSi.

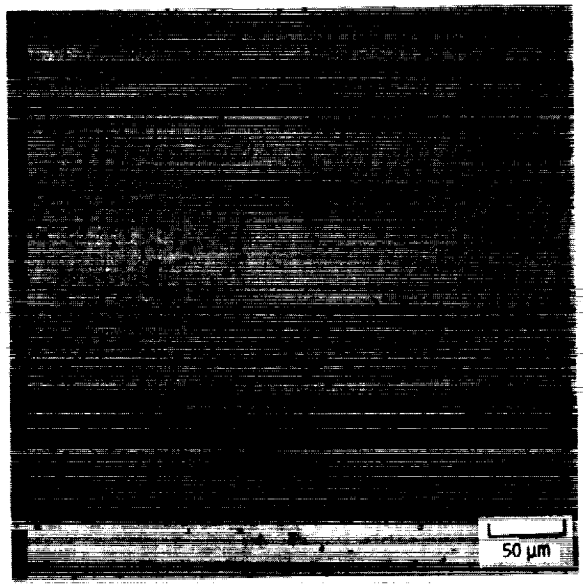

(c) ZrO_2(PSZ).

FIGURE 4. - PHOTOMICROGRAPHS OF POLISHED AND UNETCHED OXIDE CERAMIC RUB BLOCKS.

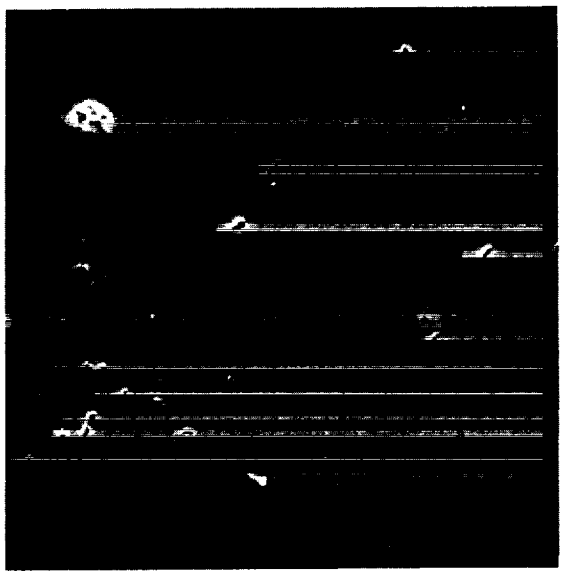

(a) Al_2O_3 (0 vol% SiC whiskers) sintered polycrystalline αAl_2O_3).

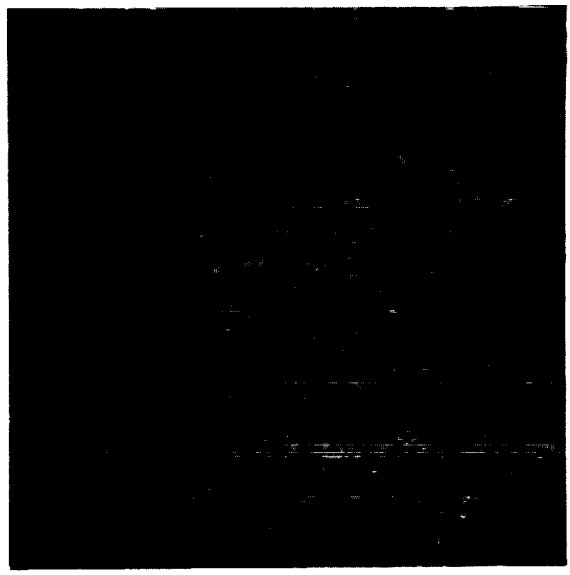

(b) Al_2O_3 (8 vol% SiC whiskers) (sintered).

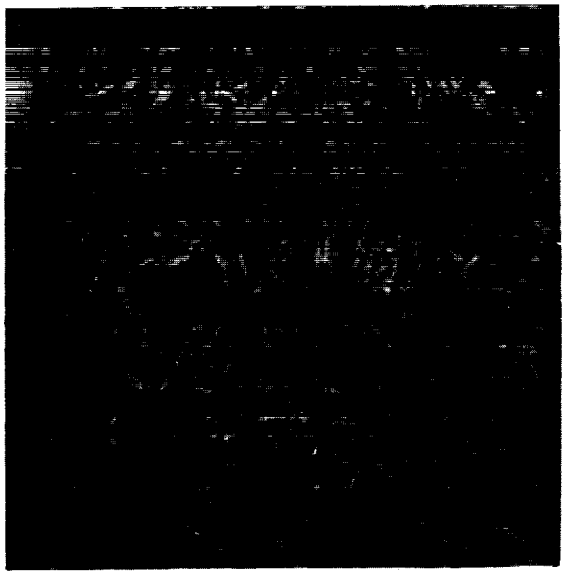

(c) Al_2O_3 (15 vol% SiC whiskers) hot pressed.

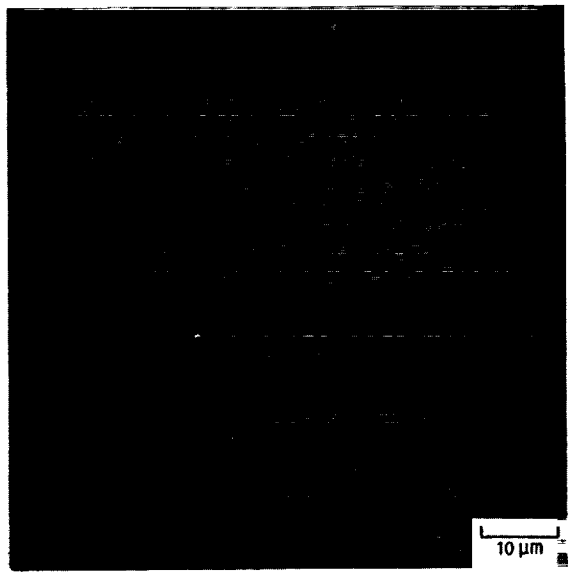

(d) Al_2O_3 (25 vol% SiC whiskers) hot pressed.

FIGURE 5. - PHOTOMICROGRAPHS OF SiC WHISKER REINFORCED Al_2O_3. POLISHED AND UNETCHED. BEFORE TEST.

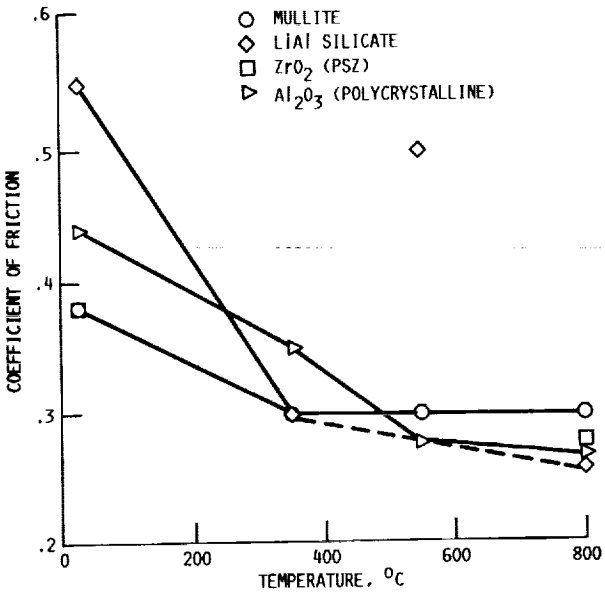

FIGURE 6. - COEFFICIENT OF FICTION VS. TEMPERATURE FOR OXIDE-CERAMICS SLIDING ON IN-718 AT A LOAD OF 67 N AND A VELOCITY OF 0.5 M/SEC.

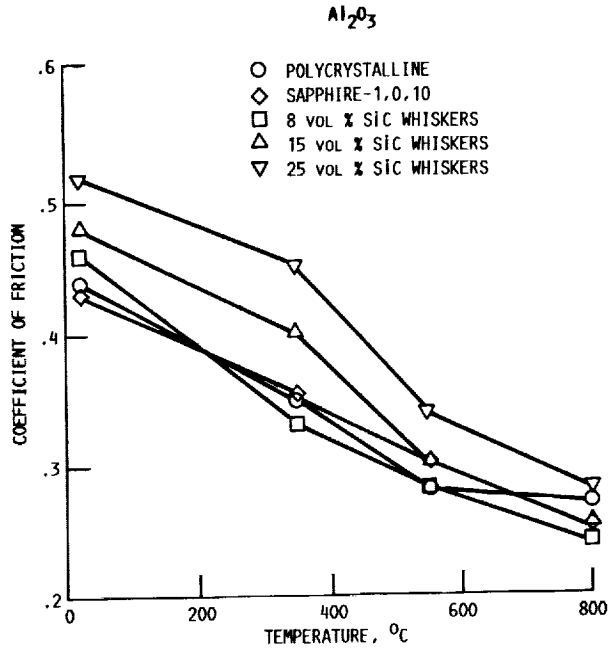

FIGURE 7. - COEFFICIENT OF FRICTION IS. TEMPERATURE FOR Al_2O_3 CERAMICS SLIDING ON IN-718 AT 67 N LOAD AND 0.5 M/SEC SLIDING VELOCITY.

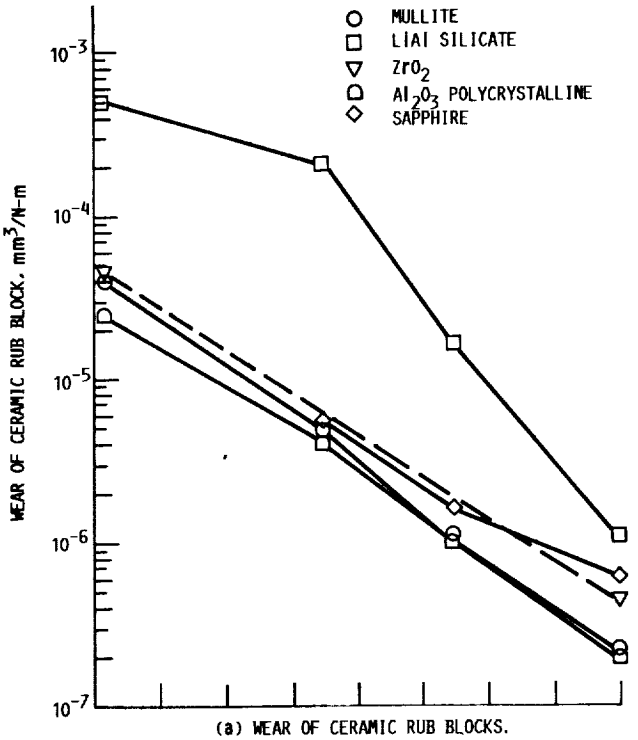

(a) WEAR OF CERAMIC RUB BLOCKS.

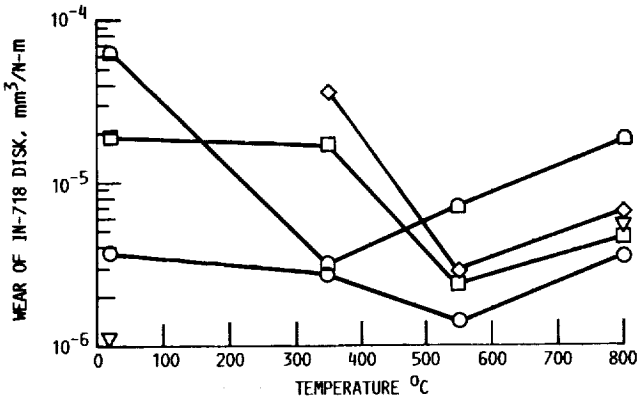

(b) WEAR OF THE IN-718 DISK.

FIGURE 8. - WEAR OF THE CERAMIC RUB BLOCKS AND IN-718 DISKS SLIDING AT A LOAD OF 67N AND VELOCITY OF 0.5 M/SEC IN AIR.

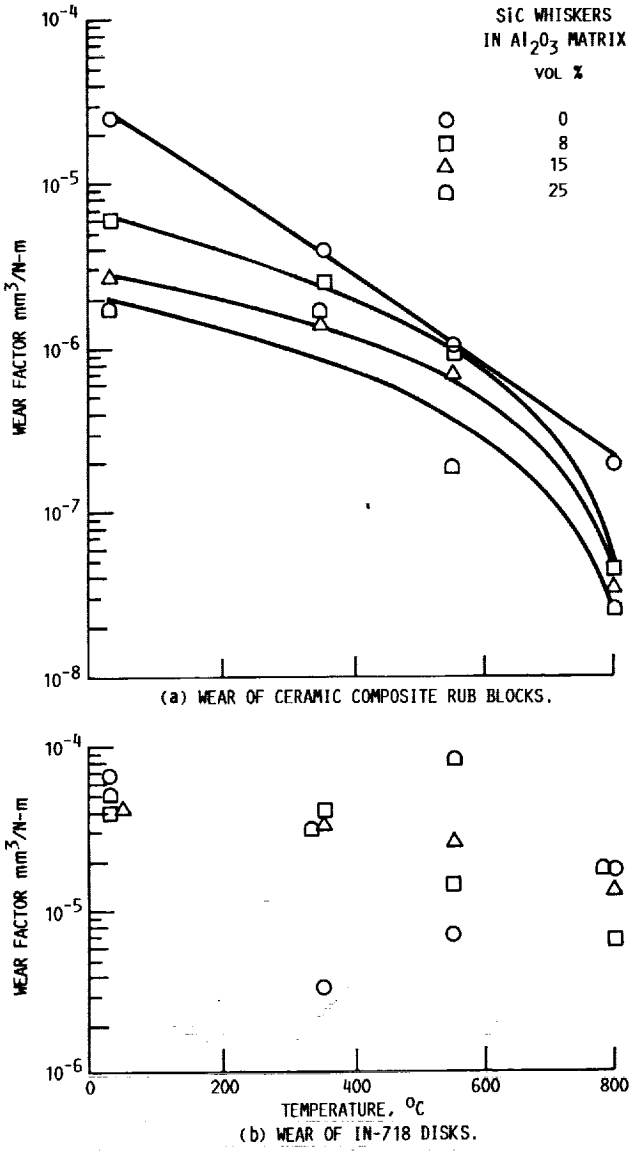

FIGURE 9. - WEAR OF COMPOSITE SiC WHISKER-REINFORCED Al_2O_3 RUB BLOCKS AND IN-718 DISKS.

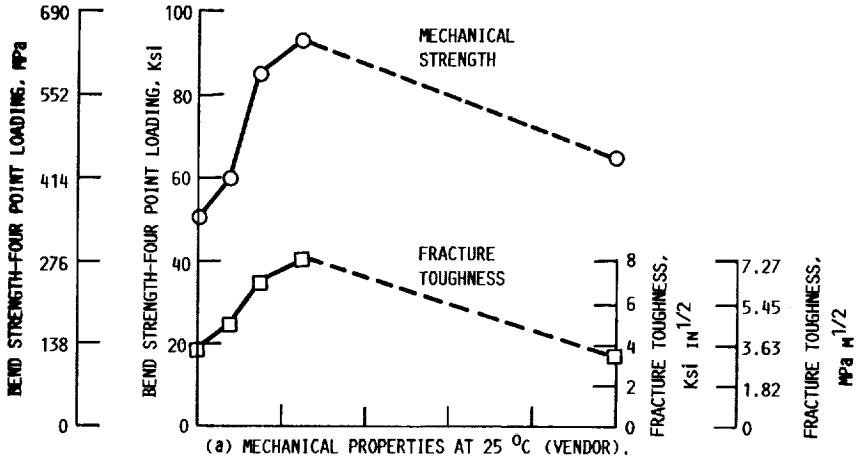

(a) MECHANICAL PROPERTIES AT 25 °C (VENDOR).

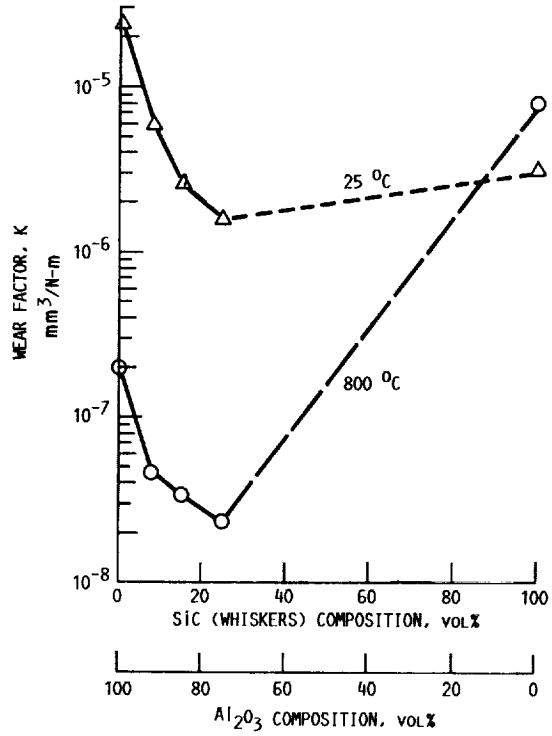

(b) WEAR FACTORS AT 25 AND 800 °C SLIDING ON IN-718 IN AIR.

FIGURE 10. - WEAR FACTOR AND MECHANICAL PROPERTIES OF SiC WHISKER REINFORCED POLYCRYSTALLINE Al_2O_3 RUB BLOCKS.

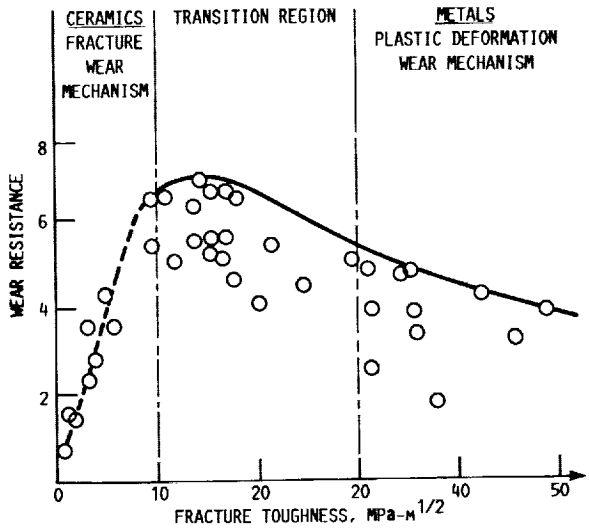

FIGURE 11. - WEAR RESISTANCE OF CERAMICS AND METALS AS A FUNCTION OF FRACTURE TOUGHNESS REF. 6.7.

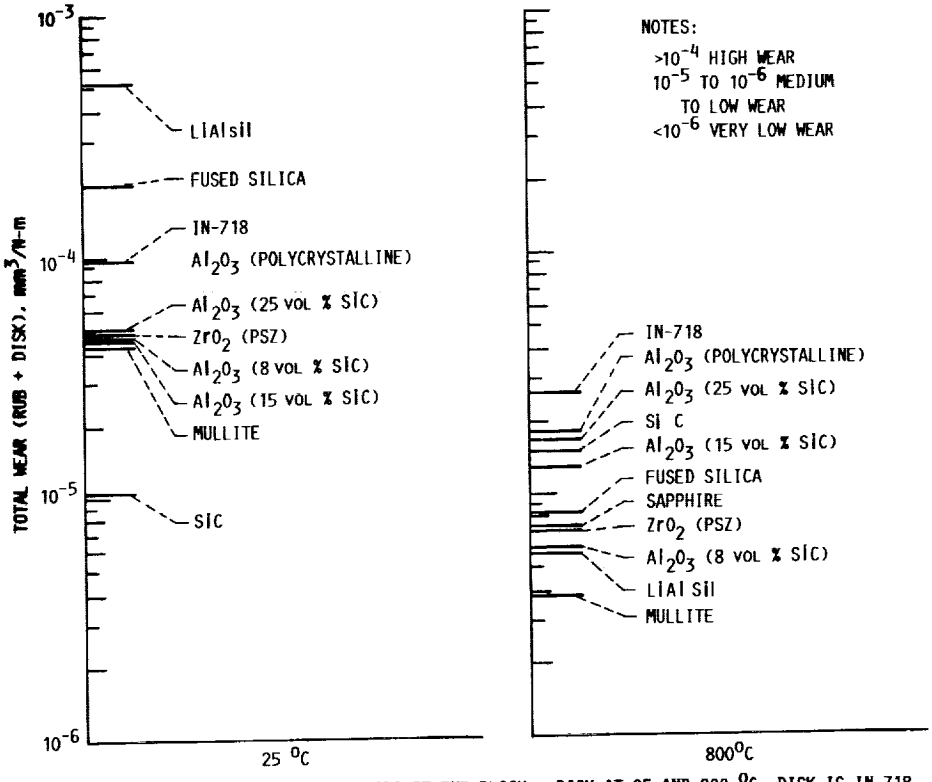

FIGURE 12. - TOTAL WEAR FACTORS OF RUB BLOCK + DISK AT 25 AND 800 °C, DISK IS IN-718 ALLOY. SLIDING LOAD 67 N AND VELOCITY IS 0.5 M/SEC.

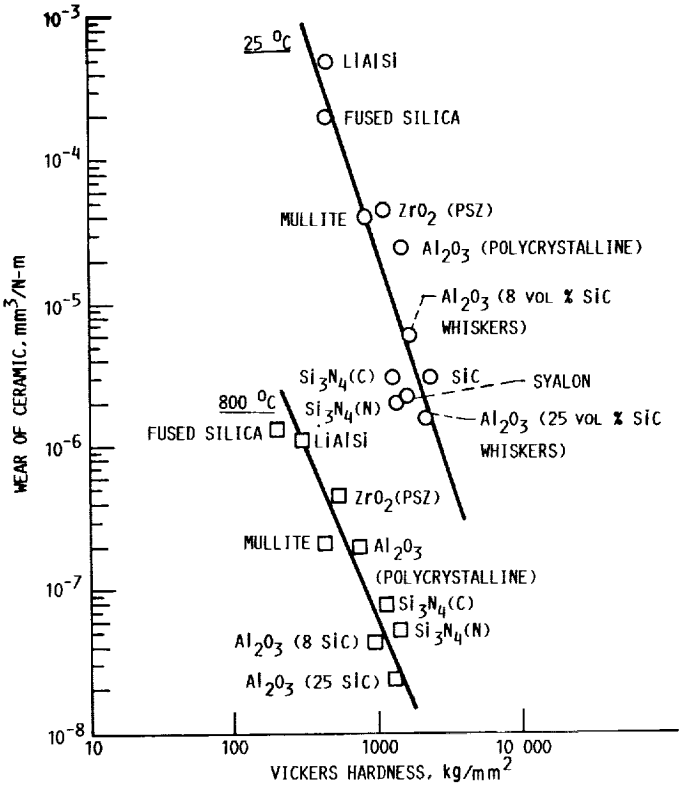

FIGURE 13. - WEAR OF THE CERAMIC RUB BLOCKS SLIDING ON IN-718 ALLOY IN AIR AT 25 AND 800 °C AT A LOAD OF 67 N FOR 60 MIN AS A FUNCTION THE VICKERS MICRO HARDNESS OF THE CERAMIC. LINES ARE LEAST SQUARES REGRESSION FITS TO DATA SETS.

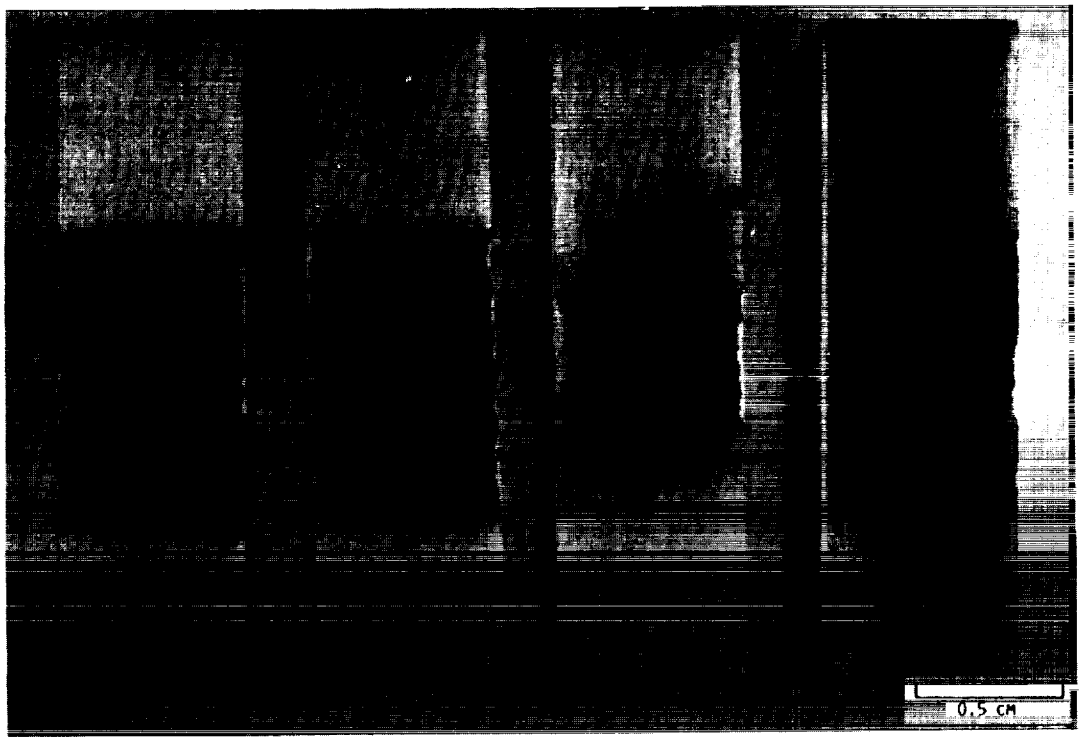

25 350 550 800 °C

FIGURE 14. - PHOTOGRAPH OF LiAlSi1. RUB BLOCKS AFTER SLIDING TEST.

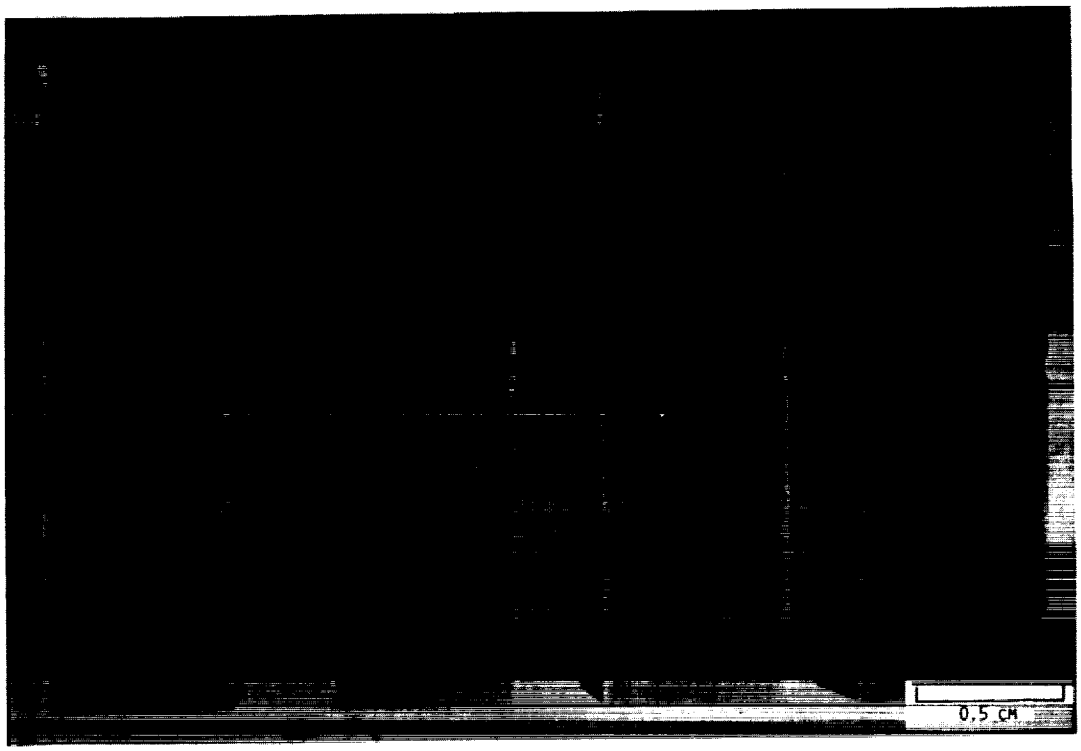

25 350 550 800 °C

FIGURE 15. - PHOTOGRAPH OF MULLITE RUB BLOCKS AFTER SLIDING TEST.

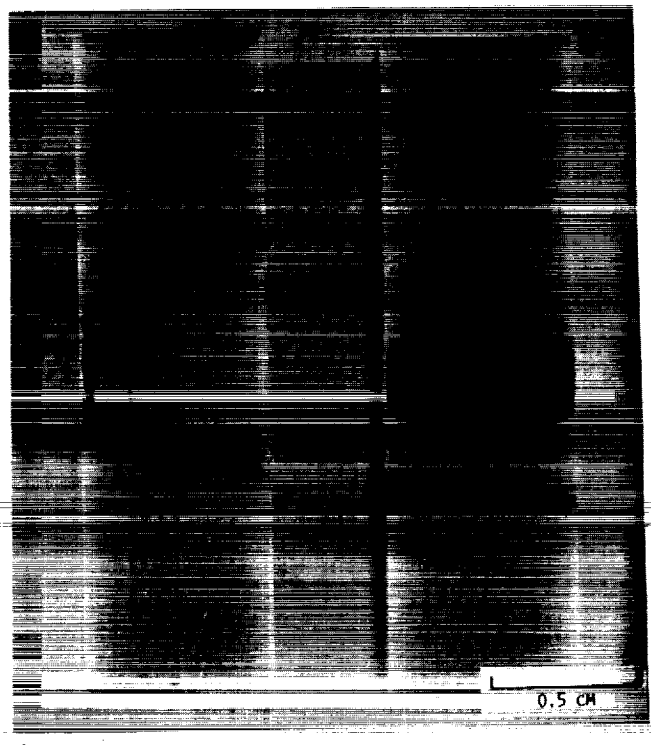

25 800 °C

FIGURE 16. - PHOTOGRAPH OF ZrO_2 (PSZ) BLOCKS AFTER SLIDING TESTS.

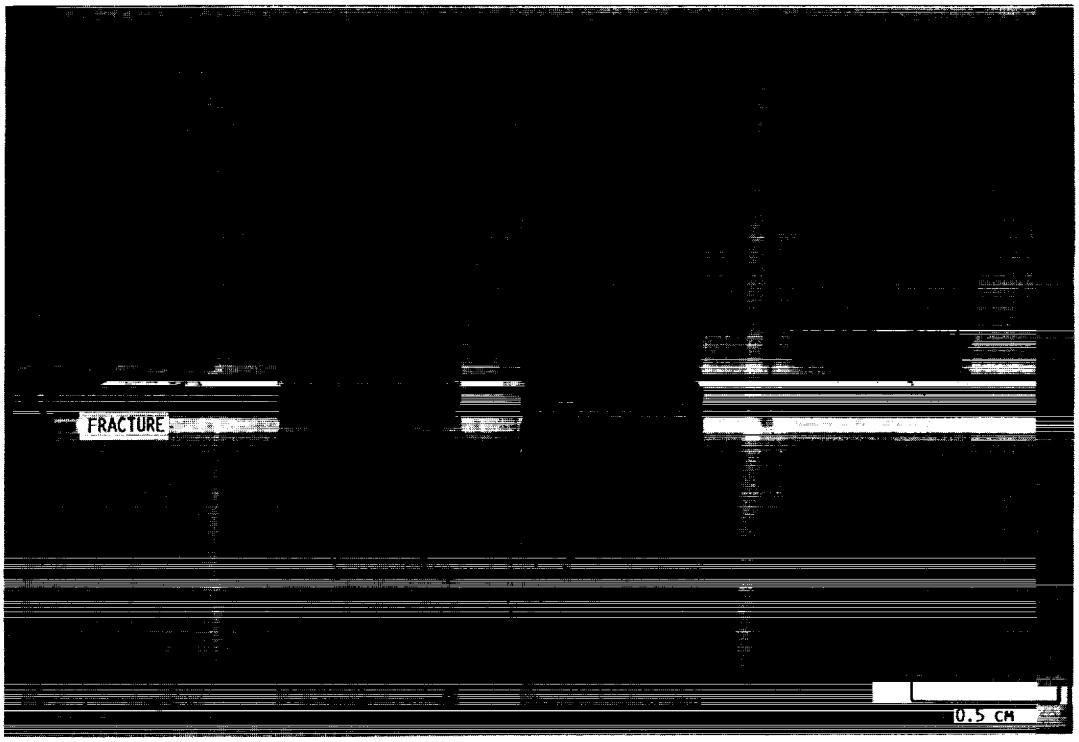

25 350 550 800 °C

FIGURE 17. - PHOTOGRAPH OF SAPPHIRE RUB BLOCKS AFTER SLIDING TEST.

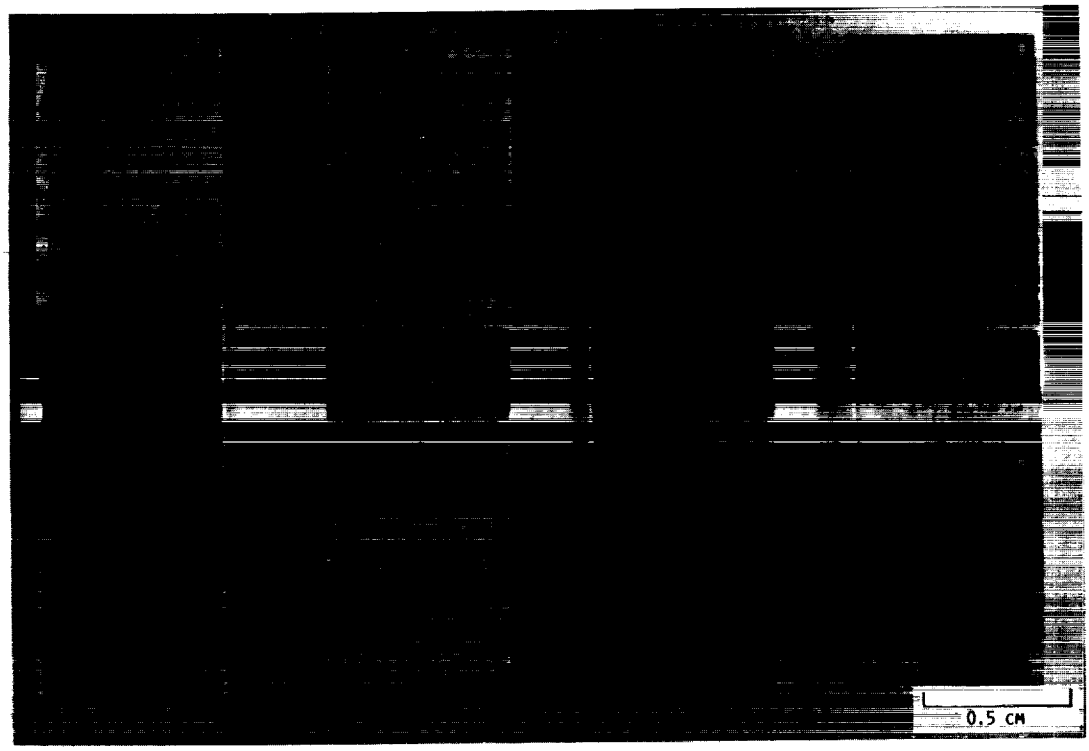

25 350 550 800 °C

FIGURE 18. - PHOTOGRAPH OF Al_2O_3 (POLYCRYSTALLINE) RUB BLOCKS AFTER SLIDING TEST.

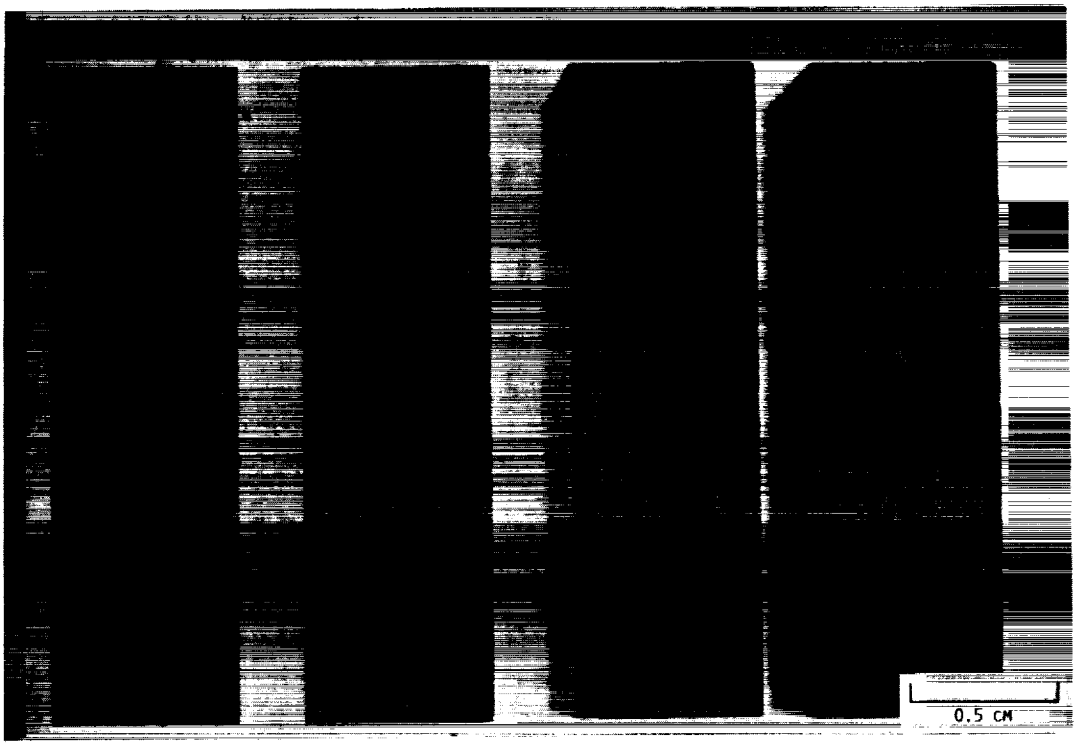

25 350 550 800 °C

FIGURE 19. - PHOTOGRAPH OF Al_2O_3 (8 VOL % SiC) RUB BLOCKS AFTER SLIDING TEST.

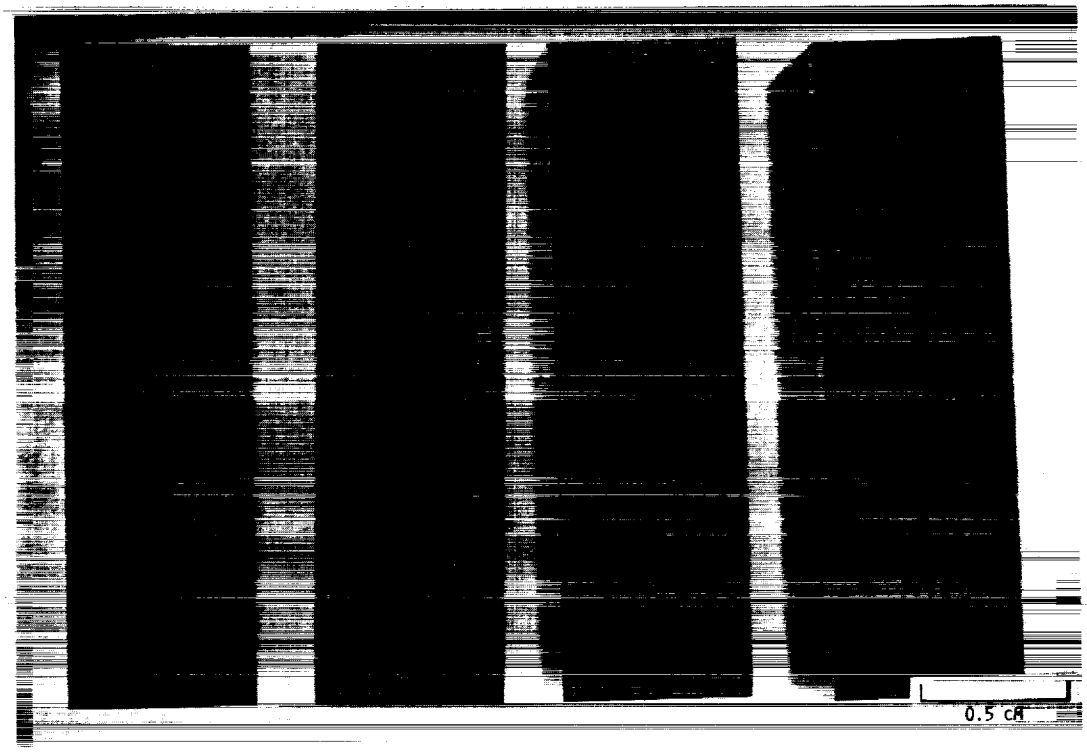

25 350 550 800 °C

FIGURE 20. - PHOTOGRAPH OF Al_2O_3 (15 VOL % SiC) RUB AFTER SLIDING TESTS.

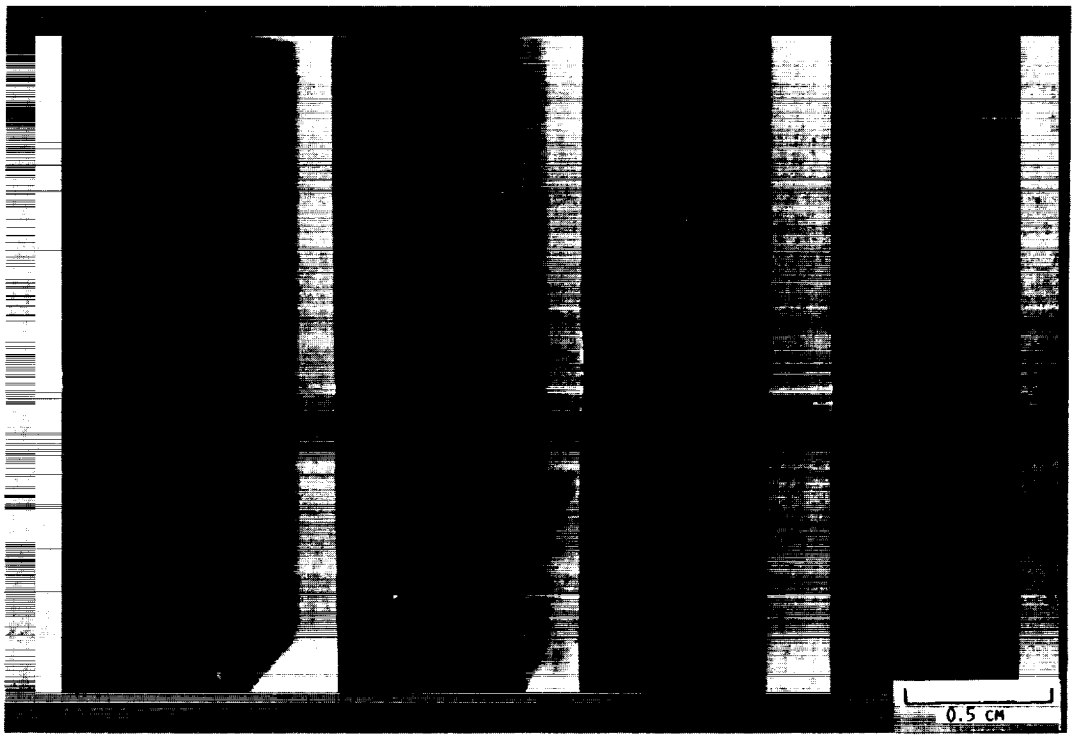

25 350 550 800 °C

FIGURE 21. - PHOTOGRAPH OF Al_2O_3 (25 vol % SiC) RUB BLOCKS AFTER SLIDING TESTS.

NASA National Aeronautics and Space Administration

Report Documentation Page

1. Report No.	2. Government Accession No.	3. Recipient's Catalog No.
NASA TM-102291		

4. Title and Subtitle

Friction and Wear of Oxide-Ceramic Sliding Against IN-718 Nickel Base Alloy at 25 to 800 °C in Atmospheric Air

5. Report Date

August 1989

6. Performing Organization Code

7. Author(s)

Harold E. Sliney and Daniel L. Deadmore

8. Performing Organization Report No.

E-4963

10. Work Unit No.

506-43-11

9. Performing Organization Name and Address

National Aeronautics and Space Administration
Lewis Research Center
Cleveland, Ohio 44135-3191

11. Contract or Grant No.

13. Type of Report and Period Covered

Technical Memorandum

12. Sponsoring Agency Name and Address

National Aeronautics and Space Administration
Washington, D.C. 20546-0001

14. Sponsoring Agency Code

15. Supplementary Notes

16. Abstract

The friction and wear of oxide-ceramics sliding against the nickel base alloy IN-718 at 25 to 800 °C were measured. The oxide materials tested were mullite ($3Al_2O_3.2SiO_2$); lithium aluminum silicate ($LiAlSi_xO_y$); polycrystalline monolithic alpha alumina (α-Al_2O_3); single crystal α-Al_2O_3 (sapphire); zirconia (ZrO_2); and silicon carbide (SiC) whisker-reinforced Al_2O_3 composites. At 25 °C the mullite and zirconia had the lowest friction and the polycrystalline monolithic alumina the lowest wear. At 800 °C the Al_2O_3-8 vol/% SiC whisker composite had the lowest friction and the Al_2O_3-25 vol/% SiC composite the lowest wear. The friction of the Al_2O_3-SiC whisker composites increased with increased whisker content while the wear decreased. In general, the wear-resistance of the ceramics improve with their hardness.

17. Key Words (Suggested by Author(s))

Friction
Wear
Ceramics
Composite materials

18. Distribution Statement

Unclassified – Unlimited
Subject Category 27

19. Security Classif. (of this report)	20. Security Classif. (of this page)	21. No of pages	22. Price*
Unclassified	Unclassified	26	A03

NASA FORM 1626 OCT 86

*For sale by the National Technical Information Service, Springfield, Virginia 22161